MEDICAL SCIENCE MONITOR

ANIMAL STUDY

e-ISSN 1643-3750
© Med Sci Monit, 2015; 21: 3179-3185
DOI: 10.12659/MSM.895624

Received: 2015.08.12
Accepted: 2015.10.02
Published: 2015.10.21

Precise Delivery Into Chronic Spinal Cord Injury Syringomyelic Cysts with Magnetic Nanoparticles MRI Visualization

Authors' Contribution:
Study Design A
Data Collection B
Statistical Analysis C
Data Interpretation D
Manuscript Preparation E
Literature Search F
Funds Collection G

ABCDEFG 1,2,3 Chao Zhang
BF 3 Anna Y. Morozova
BEF 2 Maxim A. Abakumov
BD 2 Ilya L. Gubsky
EF 1 Patricia Douglas
G 1 Shiqing Feng
AG 4 Andrey S. Bryukhovetskiy
AEG 2,3 Vladimir P. Chekhonin

1 Department of Orthopedics, Tianjin Medical University General Hospital, Tianjin, P.R. China
2 Department of Medicinal Nanobiotechnology, Pirogov Russian National Research Medical University, Moscow, Russian Federation
3 Department of Basic and Applied Neurobiology, Federal Medical Research Center for Psychiatry and Narcology, Moscow, Russian Federation
4 Center for Biomedical Technologies, Federal Research and Clinical Center for Specialized Types of Medical Assistance and Medical Technologies of The Federal Medical Biological Agency, Moscow, Russian Federation

Corresponding Authors: Chao Zhang, e-mail: chaozhang2015@gmail.com; Shiqing Feng, e-mail: sqfeng@tmu.edu.cn
Source of support: The present study was sponsored by the China Scholarship Council, CSC NO. 201406940004 and the Special Program for Sino-Russian Joint Research of the Ministry of Science and Technology, China (No. 2014DFR31210). State Key Program of National Natural Science Foundation of China (81330042) and Key Program sponsored by the Tianjin Science and Technology Committee China (13RCGFSY19000), (14ZCZDSY00044)

Background: Traumatic spinal cord injury (SCI) often results in the deficiency of glia and neurons in cystic cavities. These syringomyelic cysts can prevent axonal regeneration and sprouting. Details of the mechanism of syringomyelic cyst formation are unknown and an effective treatment for overcoming syringomyelic cysts is not available.

Material/Methods: Ten adult female Wistar rats underwent contusion SCI modeling resulting in syringomyelic cyst formation. A novel method for locating the cysts was developed and employed. MRI safe silver needles were inserted through the erector spinae of anesthetized rats to create a stable reference point. MRI images of the rodent spine were taken with the needles *in situ*. This information was used to accurately locate the cyst and determine the 3-dimensional entry point coordinates for nanoparticle delivery. Nanoparticles were injected into the cyst during a primary injection of 8 ul and a secondary injection of 8 ul, to prove the procedure can be accurately repeated.

Results: None of the rats died intra- or post-operatively. The syringomyelic cysts were accurately located with the 3-dimensional entry point coordinates. After nanoparticle delivery twice into each rat, the visualized syringomyelic cyst volume significantly decreased from 5.71±0.21 mm^3 to 3.23±0.364 mm^3 and to 1.48±0.722 mm^3.

Conclusions: The present study describes a novel strategy for precise nanoparticle delivery into a syringomyelic cyst, using measurements obtained from MRI images. This strategy may aid in developing a new method for studying chronic spinal cord injury and a novel treatment for syringomyelic cysts.

MeSH Keywords: Cell Transplantation • Magnetic Resonance Imaging • Magnetite Nanoparticles • Spinal Cord Injuries

Full-text PDF: http://www.medscimonit.com/abstract/index/idArt/895624

2061 — 5 27

Indexed in: [Current Contents/Clinical Medicine] [SCI Expanded] [ISI Alerting System] [ISI Journals Master List] [Index Medicus/MEDLINE] [EMBASE/Excerpta Medica] [Chemical Abstracts/CAS] [Index Copernicus]

Background

Six million people worldwide have spinal cord injury (SCI), most of whom are young [1]. Due to post-injury pathological processes, traumatic SCI results in cystic cavities, which can be deficient in glia and neurons [1,2]. Syringomyelic cyst capsules are formed by astrocytes, fibroblasts, ependymal cells, and collagen fibers and they exhibit neither uniform composition nor thickness [3]. These syringomyelic cysts are able to gradually elongate and expand after injury. It is widely accepted that endogenous factors, including syringomyelic cyst formation, prevent both the regeneration and sprouting of axon and compress the nerve fibers that deliver the impulses from the brain to the extremities [4–6].

In most human patients, spinal cord syringomyelic cysts develop at 4–6 weeks after SCI [3,7]. Many clinical and experimental studies have utilized various methods for repairing acute-phase SCI [7–11]. The syringomyelic cysts seem to be "incurable" with current treatments. Thus, the number of patients suffering from chronic SCI increases every year.

There is a heated debate on whether the syringomyelic cyst formation limits axonal regeneration and sprouting. To find the answer, a number of studies have been conducted *in vivo* [12–14]. After a literature review, we found there is no promising strategy for studying or overcoming post-SCI syringomyelic cysts in any animal model, including rodents, which are widely utilized by researchers.

Several approaches for the delivery of material or drugs into the exposed spinal cord were reported. These techniques include lesion site delivery [14], multi-target point delivery [15], and single-point with various intervals delivery [16]. A satisfactory strategy for locating the cysts after SCI is not currently available. None of the aforementioned approaches could be repeated accurately in a single individual. As we assessed, the rodent thoracic spinal cord is 0.1–0.3 cm in diameter and the cysts created in this narrow space are minuscule. This situation leads to a low success rate of precise location and delivery. Thus, a reliable strategy for syringomyelic cyst delivery *in vivo* is desirable.

The present study describes a novel strategy for the precise delivery into syringomyelic cysts using a magnetic resonance imaging (MRI) system. This strategy may aid in developing both a new method for studying chronic spinal cord injury and a novel treatment for the syringomyelic cysts.

Material and Methods

Animals

Experiments were carried out in compliance with the principles of International Laboratory Animal Care, and were approved by the Ethics Committee of Pirogov Russian National Research Medical University, and the European Communities Council Directive of 24 November 1986 (86/609/EEC). All efforts were made to minimize the number of animals used and their suffering. In advance of the study, 10 adult female Wistar rats (180–220 g body weight) underwent contusion spinal cord injury modeling resulting in clear signs of syringomyelic cyst formation. They were kept under controlled conditions (temperature: 22°C; humidity: 40%) on a 12-h light/dark cycle with clean food and water *ad libitum*. The PSI-IH Impactor (Precision Systems and Instrumentation LLC, Fairfax, VA) was used to initiate the injury. After a satisfactory laminectomy at the T10 level, a force of 200 kilodynes was induced to impact the exposed spinal cord. The rats were randomly divided into 2 groups. Group 1 (3 rats) was used to prove the accuracy of our method by undergoing additional MRI scans to calculate the coordinates for locating the cyst, but rats were not injected with nanoparticles. Group 2 (7 rats) underwent nanoparticle delivery after using the MRI images to locate a cyst and then to calculate the volume change of the cyst after nanoparticle delivery. MRI scanning was performed using 7 T animal MRI scanner (ClinScan, Bruker BioSpin) on the first and the fourth week after SCI (Figure 1) to evaluate the formation of syringomyelic cysts. For coronal images, T2-weighted images in coronal plane were acquired by Turbo Spin Echo sequence with the following parameters: FOV 120×59.2 mm, base resolution 320×158, TR=3850 ms, TE=39 ms, slice thickness 1 mm, number of acquisition=1, echo train length=9. For sagittal images, T2-weighted images in sagittal plane were acquired by Turbo Spin Echo sequence with the following parameters: FOV 100×49.2 mm, base resolution 256×126, TR=3850 ms, TE=42 ms, slice thickness 1 mm, number of acquisition=3, echo train length=9.

Syringomyelic cyst entry point coordinates calculation

All rats were anesthetized throughout the whole procedure with the E-Z Anesthesia system (EZ-7000 330, PA, USA). The rats were restrained on a warm pad in the prone position. The fur over T10 was shaved and the exposed skin was sterilized. The skin and the superficial fascia, which may cause resistance, were opened along the initial laminectomy incision. Two silver acupuncture needles (Kazan medical instruments plant JSC) were inserted through the erector spinae. The needles were positioned parallel to the ground and at a 40 degree angle to the spine with 1 needle on both sides of the animal. The tips the needles were passed through the muscle and intersected

Indexed in: [Current Contents/Clinical Medicine] [SCI Expanded] [ISI Alerting System] [ISI Journals Master List] [Index Medicus/MEDLINE] [EMBASE/Excerpta Medica] [Chemical Abstracts/CAS] [Index Copernicus]

Figure 1. Sagittal T2 weighted MRI images of the glial cyst formation, in 3 rats.

each other, creating a cross-like shape (Figure 2A, 2B). A MRI was performed to calculate both the volume of the syringomyelic cyst and the 3-dimensionl (3D) coordinates using the crossed needles as a reference point. Both the lateral and the longitudinal distances between the syringomyelic cyst and the crossed needles were measured with software (MultiVox Dicom Viewer) (Figure 2C–2E). The depth of the syringomyelic cyst, in relation to the surface fascia, was also measured.

Locating the syringomyelic cyst

The 3 rats in Group 1 were used to evaluate the accuracy of the calculated coordinates. A microinjection unit (Leica Biosystems Richmond) was set to guide a third silver needle through the tissues into the syringomyelic cyst according to the calculated coordinates. An MRI was performed with the third silver needle *in situ*, to evaluate the location and precision of the insertion.

Intra-cyst delivery

Intra-cyst delivery was performed on the 7 rats of Group 2 with the help of the microinjection unit and Razel Syringe Pump (Razel scientific) system. The nanoparticles were designed as previously reported [17]. Using a 25-µl Nanofil syringe with a 33-gauge needle, 8 µl of nanoparticles were delivered into the syringomyelic cyst at 4 µl/min. After the delivery, the needle was retracted slowly over a 2-min period. A post-procedure MRI was performed to evaluate the nanoparticle placement. The volumes of the syringomyelic cyst pre- and post-delivery were compared. To prove the repeatability of the approach, each rat underwent a second nanoparticle delivery (8 µl). The post-procedure MRI was again performed to evaluate the changed volume of the syringomyelic cyst. An evaluation of the change in cyst volume was performed using the MRI images taken after each of the 2 nanoparticle injections.

Statistical analysis

Data are expressed as mean ± standard error of mean (SEM) values of the mean, median, and minimum-maximum. Differences among groups were assessed with one-way analysis of variance (ANOVA) using SPSS 17.0 statistical package (SPSS Inc., Chicago, USA). Differences were considered statistically significant when $p<0.05$.

Indexed in: [Current Contents/Clinical Medicine] [SCI Expanded] [ISI Alerting System] [ISI Journals Master List] [Index Medicus/MEDLINE] [EMBASE/Excerpta Medica] [Chemical Abstracts/CAS] [Index Copernicus]

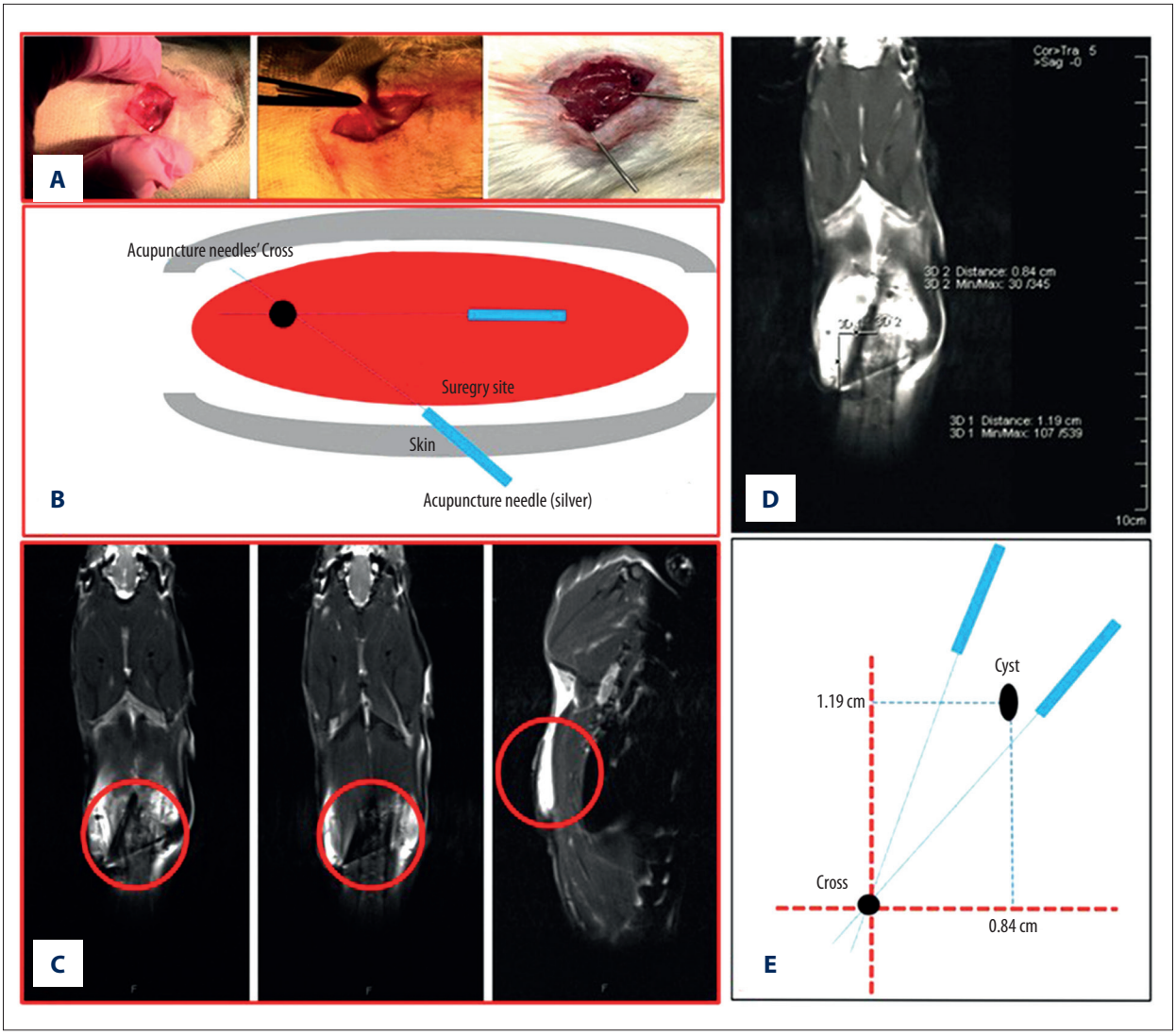

Figure 2. The calculation of the cyst entry point coordinates. (**A**) The skin and the superficial fascia were opened along the original incision. Two silver acupuncture needles were horizontally inserted into the erector spinae. (**B**) The method illustration for crossing the 2 acupuncture needles. (**C**) T2-weighted MRI images show the crossed needles. (**D, E**) The calculation of the glial cyst entry point coordinates.

Results

The operation, delivery, and MRI were performed by experienced surgeons and were well-tolerated by all rats. None of the rats died intra- or post-operatively.

Syringomyelic cyst character

The average volume of the syringomyelic cyst was 5.71±0.21 mm^3. The formation of the syringomyelic cyst presented differently in each individual (Figure 3). Three main classes were observed: 5 rats showed the sign of class 1 (50%), with the appearance of single cyst in the lesion site; 3 rats showed the sign of class 2 (30%), with the appearance of 2 separated cysts with similar size in the lesion site; and 2 rats showed the sign of class 3 (20%), with the appearance of several small cysts in the lesion site.

Syringomyelic cyst locating

The third silver acupuncture needle, introduced into the rats of Group 1, was clearly observed in the cyst in the MRI results (Figure 4). Syringomyelic cysts were effectively located with the 3D coordinates.

Intra-cyst delivery

Nanoparticle delivery was successfully performed twice in the rats of Group 2. As shown in Figure 5, the visualized

Indexed in: [Current Contents/Clinical Medicine] [SCI Expanded] [ISI Alerting System] [ISI Journals Master List] [Index Medicus/MEDLINE] [EMBASE/Excerpta Medica] [Chemical Abstracts/CAS] [Index Copernicus]

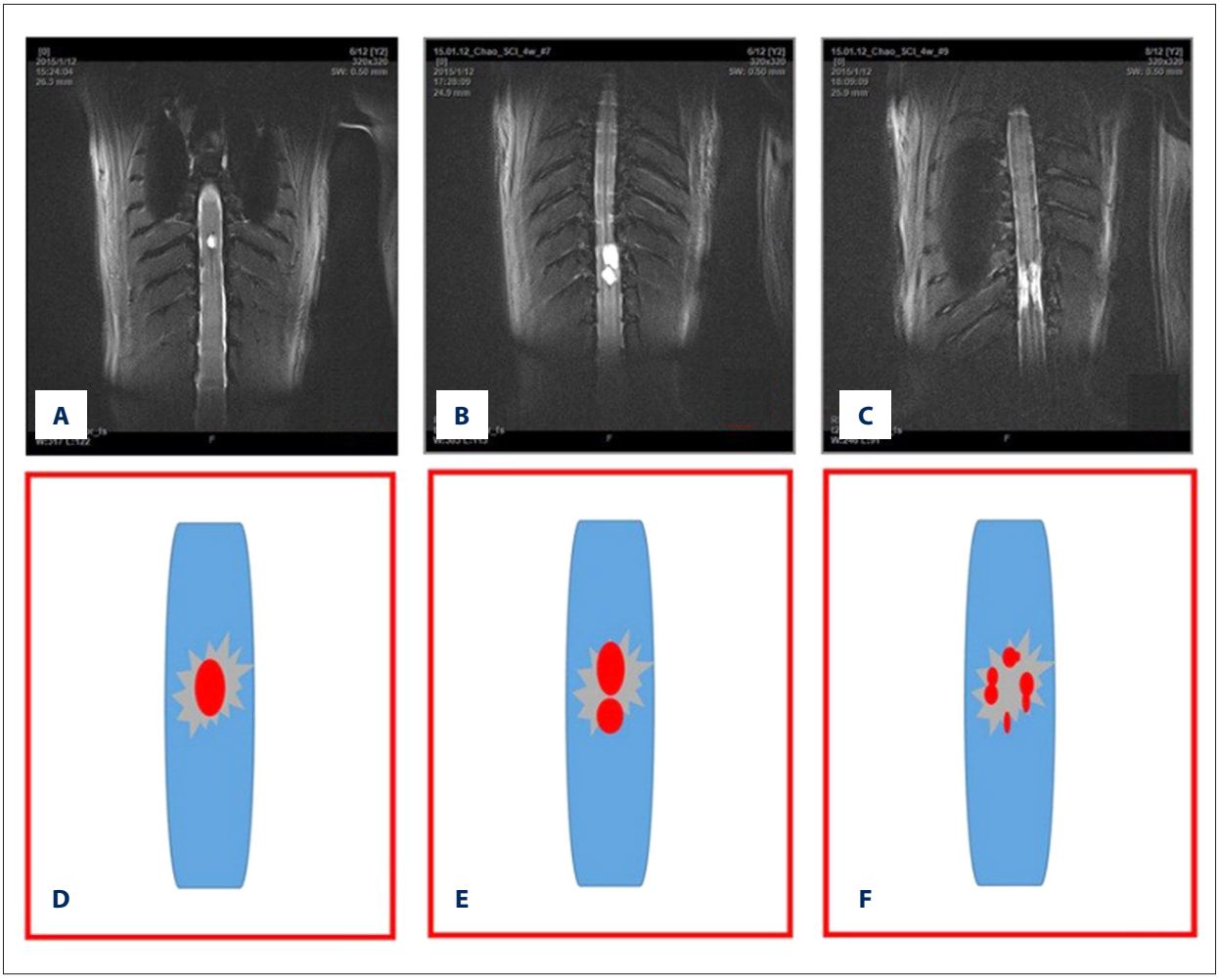

Figure 3. Three types of syringomyelic cysts seen in the specimens used in the present study. Illustration of different characters of the cysts.

syringomyelic cyst volume showed a significant change – it decreased from 5.71±0.21 mm^3 pre-delivery to 3.23±0.364 mm^3 after the first delivery ($p<0.05$). The volume further decreased significantly from 3.23±0.364 mm^3 to 1.48±0.722 mm^3 after the second delivery ($p<0.05$).

Discussion

Wound healing in the spinal cord after SCI can result in the formation of syringomyelic cysts. The detailed mechanism of the formation of syringomyelic cyst remains poorly understood.

Some researchers believe the syringomyelic cysts lead to a lack of axonal regeneration and sprouting [4]. Efforts have been made to overcome the barrier effect caused by the syringomyelic cyst. A previous report suggested a surgical approach for spinal cord cyst management. Surgical management carries a high risk of re-injuring the newly regenerated axons [18]. We doubt the risk out-weighs the possible benefit. Cell transplantation has achieved a certain level of success in both clinical and experimental studies, even though its detailed mechanism is still unknown [14,19]. Clinical reports suggest possible approaches to transplant stem cells into the syringomyelic cyst cavity [19]. However, due to the narrow structure of the rodent's spinal cord, this strategy has not been successfully conducted in rats or mice. According to our literature review, the present study is the first to describe a reproducible and precise delivery approach into the syringomyelic cyst cavity in an animal model.

The syringomyelic cyst formation is thought to be related to the central canal dilation and ependymal region disruption, which can lead to excess CSF fluid in the injury area [20]. The syringomyelic cyst gradually forms after the accumulation of CSF and the maturing of the outer capsule [20]. The outer capsule is scar tissue, consisting of a glial scar enveloping parenchyma with fibrous scar tissue in the core [21]. Glial fibrillary

Indexed in: [Current Contents/Clinical Medicine] [SCI Expanded] [ISI Alerting System] [ISI Journals Master List] [Index Medicus/MEDLINE] [EMBASE/Excerpta Medica] [Chemical Abstracts/CAS] [Index Copernicus]

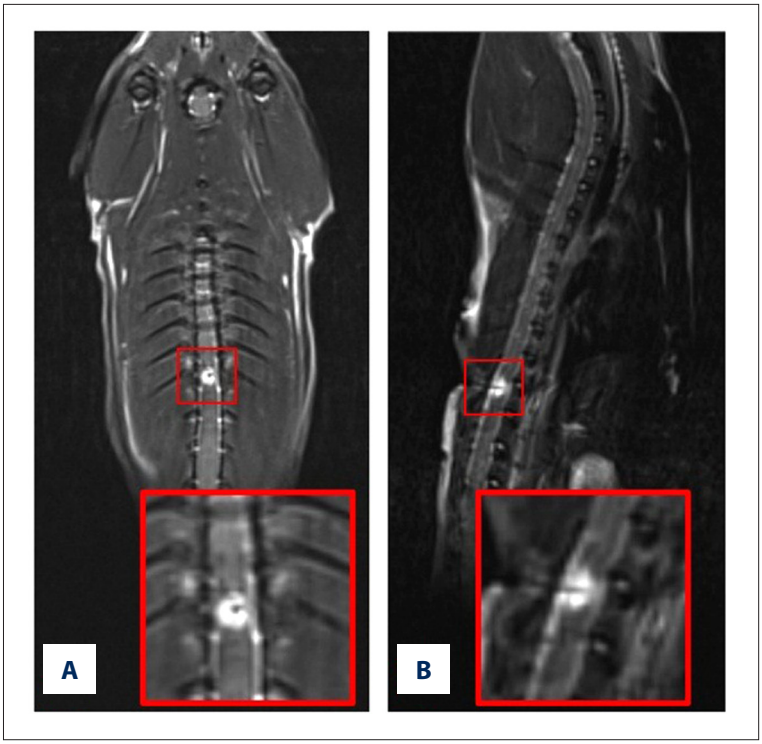

Figure 4. The coronal (**A**) and sagittal (**B**) T2-weighted MRI images showing the silver acupuncture needle marking the location of the cyst.

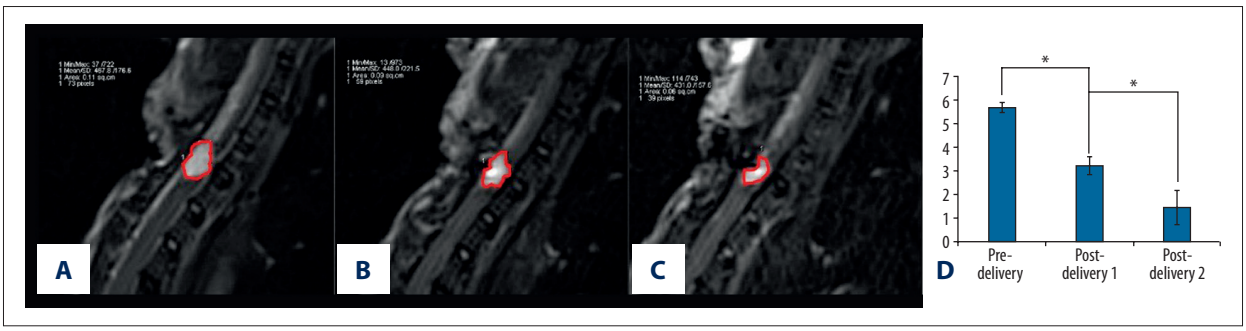

Figure 5. The volume change of syringomyelic cyst post nanoparticle transplantation. The volume of syringomyelic cyst decreased after the first delivery, and further decreased after the second delivery, and further decreased after the second delivery (* $p<0.05$).

acidic protein (GFAP) is over-expressed by reactive astrocytes that compose the capsule [22,23]. The lesion core consists of collagen IV [21]. It is widely accepted by surgeons that the optimal strategy for stem cells therapy is intra-syringomyelic cyst delivery of the cells. Conversely, most of the current basic research employs lesion site delivery [14], multi-target point delivery [15], and single-point with various intervals delivery [16] methods. We hypothesized that efficacy of the cell transplantation is affected by the unique composition of each syringomyelic cyst capsule and the variation of fluid pressure within the cyst.

In the present study, we used magnetic nanoparticles as the transplantation substance. The magnetic nanoparticles are known to be a negative contrast agent for the MRI due to their super-paramagnetic properties. After intra-cyst injection, the nanoparticles spread inside the cyst and they appeared as a dark area in T2-weighted MRI, masking the real volume of the cyst. In this case we did not reduce the actual volume of the cyst, but just visualized the injection site and total volume. Thus, the volume further decreased significantly after the second delivery, suggesting the present approach is reproducible. MRI imaging is necessary for evaluating the contusion after SCI in the animal model, as lesion sites can be accurately evaluated and measured with this diagnostic method. In our experiences, syringomyelic cysts occur in various areas of the spinal volume, even when all models are created by the same surgeon and using the same well calibrated electrical impactor. Syringomyelic cysts can differ in shape and quantity in each individual (Figure 1, Figure 3). It was reported that the most important clinical sign of syringomyelia is pain [24,25]; other neurological deficits, including thoracic-limb weakness, muscle atrophy, and pelvic limb ataxia and weakness, were also

Indexed in: [Current Contents/Clinical Medicine] [SCI Expanded] [ISI Alerting System] [ISI Journals Master List] [Index Medicus/MEDLINE] [EMBASE/Excerpta Medica] [Chemical Abstracts/CAS] [Index Copernicus]

observed [25,26]. At present, the literature suggests that signs of pain are not well correlated with the size of the syringomyelia [27]. However, few papers focussed on the detailed correlation between the character of the syringomyelic cyst and the ability of SCI patients to recover function after injury. We can at least infer that the when less space is occupied by syringomyelic cysts in the chronic injury lesion site, there is more space for the injured axons to sprout and possibly re-connect.

Conclusions

We described an approach that can be used for precise drug, nanomaterial, scaffold, antibody, and biomarker delivery *in vivo* research. We believe it will be a reliable approach for repairing the syringomyelic cyst, and also for studying chronic spinal cord injury.

Acknowledgements

We thank Alevtina T. Syomkina's for preparing the nanoparticles, and Ionova K.P. and Zubkov E.A. for taking care of the animals.

Conflict of interest

The authors declare that they have no conflict of interest.

References:

1. McDonald JW, Sadowsky C: Spinal-cord injury. Lancet, 2002; 359: 17–425
2. Dumont RJ, Okonkwo DO, Verma S et al: Acute spinal cord injury, part I: pathophysiologic mechanisms. Clin Neuropharmacol, 2001; 24: 254–64
3. Guizar-Sahagun G, Grijalva I, Madrazo I et al: Development of post-traumatic cysts in the spinal cord of rats-subjected to severe spinal cord contusion. Surg Neurol, 1994; 41: 241–49
4. Young W: Spinal cord regeneration. Cell Transplant, 2014; 23: 573–611
5. Hodgetts SI, Simmons PJ, Plant GW: A comparison of the behavioral and anatomical outcomes in sub-acute and chronic spinal cord injury models following treatment with human mesenchymal precursor cell transplantation and recombinant decorin. Exp Neurol, 2013; 248: 343–59
6. Kim K, Mishina M, Kokubo R et al: Ketamine for acute neuropathic pain in patients with spinal cord injury. J Clin Neurosci, 2013; 20(6): 804–7
7. Boido M, Garbossa D, Fontanella M et al: Mesenchymal stem cell transplantation reduces glial cyst and improves functional outcome after spinal cord compression. World Neurosurg, 2014; 81: 183–90
8. Macaya DJ, Hayakawa K, Arai K, Specotr M: Astrocyte infiltration into injectable collagen-based hydrogels containing FGF-2 to treat spinal cord injury. Biomaterials, 2013; 34: 3591–602
9. Qi YH, Yao WL, Zhang CH, Guo YQ: Effect of lentivirus-mediated RNA interference of APC-Cdh1 expression on spinal cord injury in rats. Genet Mol Res, 2014; 13: 1366–72
10. Zhao RR, Andrews MR, Wang D et al: Combination treatment with anti-Nogo-A and chondroitinase ABC is more effective than single treatments at enhancing functional recovery after spinal cord injury. Eur J Neurosci, 2013; 38: 2946–61
11. Wang T, Yuan W, Liu Y et al: miR-142-3p is a potential therapeutic target for sensory function recovery of spinal cord injury. Med Sci Monit, 2015; 21: 2553–56
12. Hu Z, Tu J: The roads to mitochondrial dysfunction in a rat model of post-traumatic syringomyelia. Biomed Res Int, 2015; 2015: 831490
13. Wang F, Qi HX, Zu Z et al: Multiparametric MRI reveals dynamic changes in molecular signatures of injured spinal cord in monkeys. Magn Reson Med. 2015; 74(4): 1125–37
14. Mannoji C, Koda M, Kamiya K et al: Transplantation of human bone marrow stromal cell-derived neuroregenrative cells promotes functional recovery after spinal cord injury in mice. Acta Neurobiol Exp (Wars), 2014; 74: 479–88
15. Rao YJ, Zhu WX, Du ZQ et al: Effectiveness of olfactory ensheathing cell transplantation for treatment of spinal cord injury. Genet Mol Res, 2014; 13: 4124–29
16. Cigognini D, Satta A, Colleoni B et al: Evaluation of early and late effects into the acute spinal cord injury of an injectable functionalized self-assembling scaffold. PLoS One, 2011; 6: e19782
17. Abakumov MA, Shein SA, Vishvasrao H et al: Visualization of experimental glioma C6 by MRI with magnetic nanoparticles conjugated with monoclonal antibodies to vascular endothelial growth factor. Bull Exp Biol Med, 2012; 154: 274–77
18. Edgar RE: Surgical management of spinal cord cysts. Paraplegia, 1976; 14: 21–27
19. Al-Zoubi A, Jafar E, Jamous M et al: Transplantation of purified autologous leukapheresis-derived CD34(+) and CD133(+) stem cells for patients with chronic spinal cord injuries: long-term evaluation of safety and efficacy. Cell Transplant, 2014; 1: 25–34
20. Gardner WJ, Goodall RJ: The surgical treatment of Arnold Chiari malformation in adults. An explanation of its mechanism and importance of encephalography in diagnosis. J Neurosurg, 1950; 7: 199–206
21. Silver J, Miller JH: Regeneration beyond the glial scar. Nat Rev Neurosci, 2004; 5: 146–56
22. Kim MS, Kim SH: Syringomyelia associated with a spinal arachnoid cyst. J Korean Neurosurg Soc, 2009; 45: 315–17
23. Ben Haim L, Carrillo-de Sauvage MA, Ceyzériat K, Escartin C: Elusive roles for reactive astrocytes in neurodegenerative diseases. Front Cell Neurosci, 2015; 9: 278
24. Nakamura M, Chiba K, Nishizawa T et al: Retrospective study of surgery-related outcomes in patients with syringomyelia associated with Chiari I malformation: Clinical significance of changes in the size and localization of syrinx on pain relief. J Neurosurg, 2004(3 Suppl. Spine): 241–44
25. Todor DR, Harrison TM, Millport TH: Pain and syringomyelia: A review. Neurosurg Focus, 2000; 8: 1–6
26. Rusbridge C, MacSweeny JE, Davies JV et al: Syringomyelia in cavalier king charles spaniels. J Am Anim Hosp Assoc, 2000; 36: 34–41
27. Lu D, Lamb CR, Pfeiffer DU et al: Neurological signs and results of magnetic resonance imaging in 40 cavalier King Charles Spaniels with Chiari type 1 like malformations. Vet Rec, 2003; 153: 260–63

Indexed in: [Current Contents/Clinical Medicine] [SCI Expanded] [ISI Alerting System] [ISI Journals Master List] [Index Medicus/MEDLINE] [EMBASE/Excerpta Medica] [Chemical Abstracts/CAS] [Index Copernicus]